High-contrast imaging in wide spectral band with a self-coherent camera and achromatic coronagraphs

J.R. Delorme [a], R. Galicher[a], P. Baudoz[a], G. Rousset[a], J. Mazoyer[a],
M.N'Diaye[b], K. Dohlen[c] and A. Caillat[c]

[a] Lesia, Observatoire de Paris, CNRS and University Denis Diderot Paris 7, 5 place Jules Janssen, 92195 Meudon, France
[b] Space Telescope Science Institute, 3700 San Martin Drive, Baltimore, MD 21218, USA
[c] Laboratoire d'Astrophysique de Marseille, Université d'Aix-Marseille & CNRS, UMR 7326, 38 rue Frédéric Joliot-Curie, 13388 Marseille Cedex 13, France

ABSTRACT

Direct imaging of exoplanets is very attractive but challenging. It requires high angular resolution and very high-contrast imaging. One solution is the use of coronagraphs behind the adaptive optics of large telescopes. Unfortunately, optics of space telescope and ground telescope introduce quasi-static aberrations which strongly limit the quality of the final image and a dedicated stage of adaptive optics is required. We proposed a self-coherent camera (SCC) in 2006 and we obtained contrast levels of $\approx 2 \ 10^{-8}$ at a few λ_0/D at 638 nm in laboratory. In this paper, we explain how to achromatize the SCC. We present laboratory performance in wide spectral band $\approx 5 - 10$ % bandpass.

Keywords: High-contrast imaging – Exoplanets – Adaptive optics – Coronagraph

1. INTRODUCTION

Unlike the methods of indirect detection, direct imaging methods can characterize the atmosphere of exoplanets in the outer part of exoplanetary systems. Some young exoplanets at large separations have already been detected.[1,2,3,4] The main challenge of direct imaging is the high-contrast level required to extract the planet signal from the stellar light.

To reach high-contrast, coronagraphs are commonly proposed. They can theoreticaly reject all the stellar light. However, their performance are strongly limited by wavefront aberrations which introduce speckles in the focal plane. One solution to overcome the speckle limitation, is the use of a DM upstream of the coronagraph.[5]

The self-coherent camera[6] (SCC) developed in our laboratory is a focal plane wavefront sensor which uses the coherence between the focal plane speckles and the stellar light rejected by the coronagraph. The technique was demonstrated using numerical simulations[7] and laboratory experiments[8] by our team. Our current laboratory performance is $\approx 10^{-8}$ in monochromatic light.[9] Mazoyer et al. 2014, showed that the first version of the SCC is efficient in quasi-monochromatic light only. This limitation has to be overcome because the association of a coronagraph, a DM and a focal plane wavefront sensor should work in broadband to obtain images of faint objects like exoplanets or disk.

Two elements in our setup are sensitive to chromatism: the four quadrant phase mask (FQPM[10]) which is the coronagraph and the SCC. For these reasons, we tested two achromatic coronagraphs, the multi four-quadrant phase-mask (MFQPM) and the dual zone phase mask (DZPM) (§3), and we upgraded the SCC (§4).

2. THE THD BENCH AND PREVIOUS PERFORMANCES

The THD bench and SCC were described in several papers[6,11,12] and, we only propose a brief reminder of the main information about the THD bench in §2.1, we remind how the SCC works in §2.2 and finally, we remind in §2.3 the performance already reached.

E-mail: jacques-robert.delorme@obspm.fr, Telephone: +33 (0)1 45 07 75 12

2.1 Presentation of THD bench

We built the THD bench in order to develop and test high-contrast imaging techniques in visible light in preparation of future instruments. It is a reflective-only bench and the main components are a supercontinuum source ($400 - 2000$ nm), a laser diode (638 nm), a tip-tilt mirror, a 32x32 Boston Micromachines deformable mirror (DM), a coronagraph and a focal plane camera used as a wavefront sensor. The bench is described in details in a previous paper.[8]

In this paper, we used several spectral filters (Table 1). The shape of the R8 spectrum was slightly different for the 2 experiments we present in this paper ($\Delta\lambda = 70$ or 80 nm). We will provide the measured spectrum in situ for each experiment.

Name of filters used	λ (nm)	$\Delta\lambda$ (nm)	Resolution $R = \frac{\lambda}{\Delta\lambda}$
Laser	638	<2	>300
620-10	615	9	70
647-10	643	9	71
660-10	657	8	80
680-10	675	8	88
R22	652	30	22
R8	641	70-80	9-8

Table 1. List of the filters used in this paper. We define $\lambda_0 = 638$ nm which is the wavelength of the laser.

2.2 Brief reminder of the SCC

In order to reduce the speckle noise, we developed a focal plane wavefront sensor called the self-coherent camera (SCC[6]). It uses the coherence between the light of the focal plane speckles and the stellar light rejected by the coronagraph. To implement the SCC, we modify the Lyot stop of the coronagraph by adding an off-axis small circular reference hole (Fig.1, Left). This hole selects part of the star light rejected by the coronagraphic mask and generates interference fringes over the speckle field in the SCC image in the focal plane because of the spatial coherence of the star light (Fig.1, middle). From the fringes, we can estimate the speckle complex electric field. Figure 1 (right) shows the Fourier transform of the focal plane SCC image. Two main structures are visible:

- The central autocorrelation peak of the Lyot stop that we do not use here (see Baudoz et al. 2006).

- The lateral correlation peaks between the reference hole and the main coronagraphic pupil.

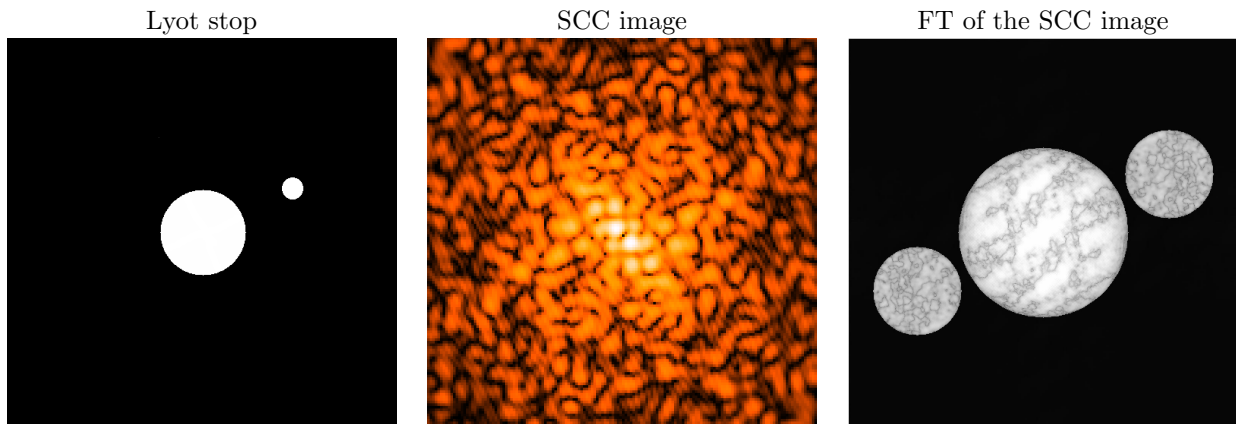Lyot stop   SCC image   FT of the SCC image

Figure 1. Left: Lyot stop with one reference and the classical Lyot stop (center). Middle: SCC image in monochromatic light. Right: Fourier transform of the SCC image.

Mazoyer et al. (2014)[8] explained how to determine the complex electric field of the speckles from the correlation peaks. Their position and their size depend on the position and the size of the reference hole in the Lyot stop plane.

We use this estimate to control the DM and minimize the speckle energy on the detector.[9]

2.3 Performance of the SCC with FQPM

Up to now, the coronagraph used on the THD bench was composed by a four quadrant phase mask (FQPM) in a focal plane and a Lyot stop in the following pupil plane. The diameter of our Lyot stop diaphragm was $\emptyset_L = 8$ mm when the entrance pupil was $\emptyset_P = 8.1$ mm. The diameter of the SCC reference was 0.35 mm and the distance between the optical axis and the center of this hole reference was $\xi = 1.8\,\emptyset_L$.

The FQPM can theoretically reject all the stellar light outside of the Lyot stop diaphragm.[13] However, due to aberrations, a part of the stellar light reaches the detector and creates speckles in the image. The SCC was expected to reach high-contrast levels from numerical simulations[7] which was demonstrated in laboratory later.[9] Left image of Figure 2 shows laboratory performance obtained in monochromatic light ($\lambda_0 = 638$ nm). We corrected only a half dark hole (DH) because we only have one DM on our bench and we corrected for both phase and amplitude aberrations.[5] In this paper, the size of all images that we show is 30 by 30 λ_0/D. We also use the same colorbar for all images inside the half DH. The rest of the image can be saturated. The central drawing gives the main dimensions of the image. The central cross represents the optical axis of the instrument which is also the position of the star and the focal plane mask position. For the image presented in Figure 2, the size of the corrected area is 10.5 by $23\lambda_0/D$ and the standard deviation inside it achives $2.4\ 10^{-8}$. The plot is the contrast defined as the azimutal standard deviation (1σ) versus angular separation in λ_0/D. We compute this contrast as describe in reference.[14] For an angular separations within the range of 5 and 12 λ_0/D, the contrast is $\approx 2\ 10^{-8}$. We cannot correct speckles with an angular separation smaller than 5 λ_0/D because of amplitude aberrations with low spatial frequencies. Moreover, the correction for angular separations greater than 12 λ_0/D is not possible because of the limited number of actuators of our DM.
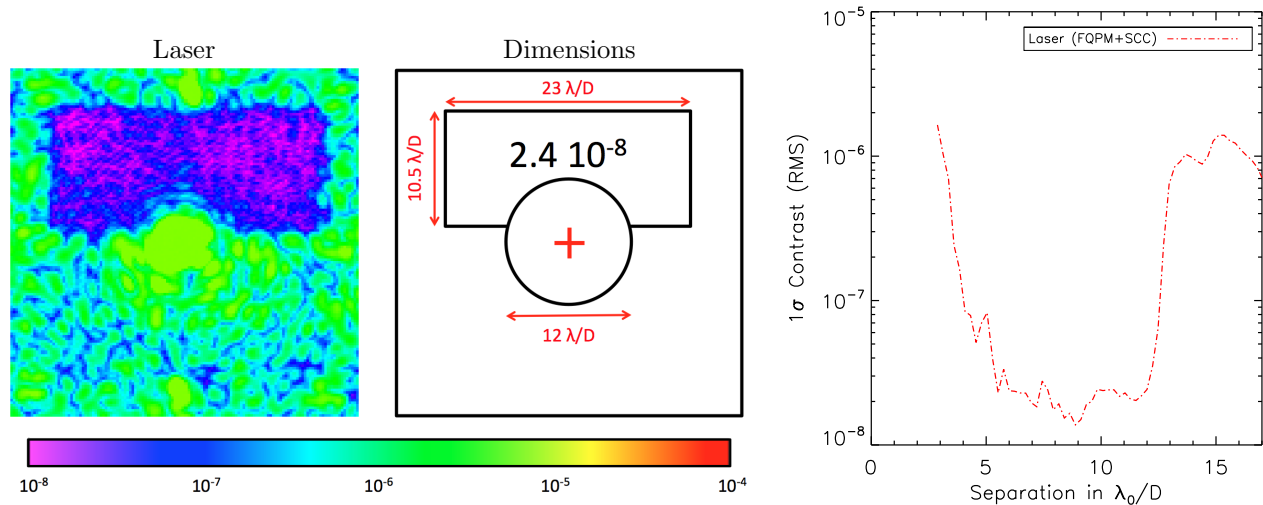

Figure 2. Left: experimental half dark hole (DH) obtained with the FQPM+SCC in monochromatic light. The size of this image is 30 by 30 λ_0/D. Middle: dimensions of the DH. The red cross represents the optical axis. The standard deviation inside the half DH is $2.4\ 10^{-8}$. Right: Associated 1σ contrast curve ($\lambda_0 = 638$ nm) computed inside the DH.

Performance in monochromatic light of the association FQPM+SCC will be taken as a reference in the following sections.

3. ACHROMATIC CORONAGRAPHS

In this part, we determine how achromatic the MFQPM and the DZPM coronagraphs are. First, we describe the protocole of the experiment in §3.1. Then, in §3.2, we write a short reminder on how the MFQPM works, and we describe its performance in polychromatic light. Finally, in §3.3, we do the same for the DZPM.

3.1 Description of the experiment

In order to compare the performance of MFQPM and DZPM and to separate chromatic effects of the coronagraphs from those of the focal plane wavefront sensor (SCC):

- First, we control the DM using the MFQPM+SCC or DZPM+SCC in monochromatic light (Laser) to minimize the speckle energy in a half DH as done previously with the FQPM+SCC (§2.2).

- Then, we record coronographic images for all the available filters without changing the DM shape.

From these images, we can study the performance of the coronagraphs as a function of wavelength and spectral bandwidth.

3.2 MFQPM

3.2.1 Brief reminder

The multi-stage four-quadrant phase mask (MFQPM) was proposed and developed by our team.[15,16] It associates several monochromatic four-quadrant phase mask coronagraphs in cascade. Our prototype (Fig. 3, Left) includes three FQPM optimized for the same wavelength $\lambda_0 = 638$ nm. From numerical simulation a contrast of 10^{-8} is expected for a spectral bandpass of $R = 8$. The filter transmission curves used for characterizing our MFQPM prototype are plotted on the right of the Figure 3.
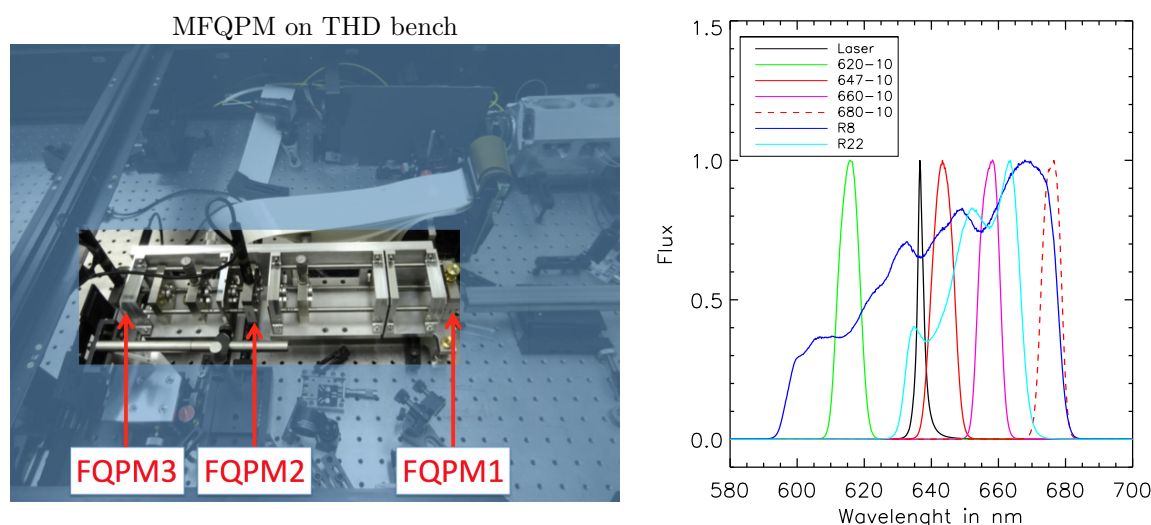

Figure 3. Left, photography of our MFQPM prototype. Right: spectra used with our MFQPM prototype.

3.2.2 Results and comments

In monochromatic light (Fig. 4), performance are close to those obtained with the FQPM: contrast of $3 \; 10^{-8}$ between 5 and $10\lambda_0/D$. Unfortunately, we did not correct the largest half DH we could (up to $13\lambda_0/D$). We used a cutoff at $10\lambda_0/D$ which explains the speckles are not corrected further. The standard deviation inside the half DH (Fig. 4) is $3.3 \; 10^{-8}$. In this experiment, the diameter of our Lyot stop diaphragm was $\varnothing_L = 7.6$ mm when the entrance pupil was $\varnothing_P = 8$ mm. The diameter of the SCC reference was 0.35 mm and the distance between the optical axis and the center of this hole reference was $\xi = 1.8 \; \varnothing_L$.
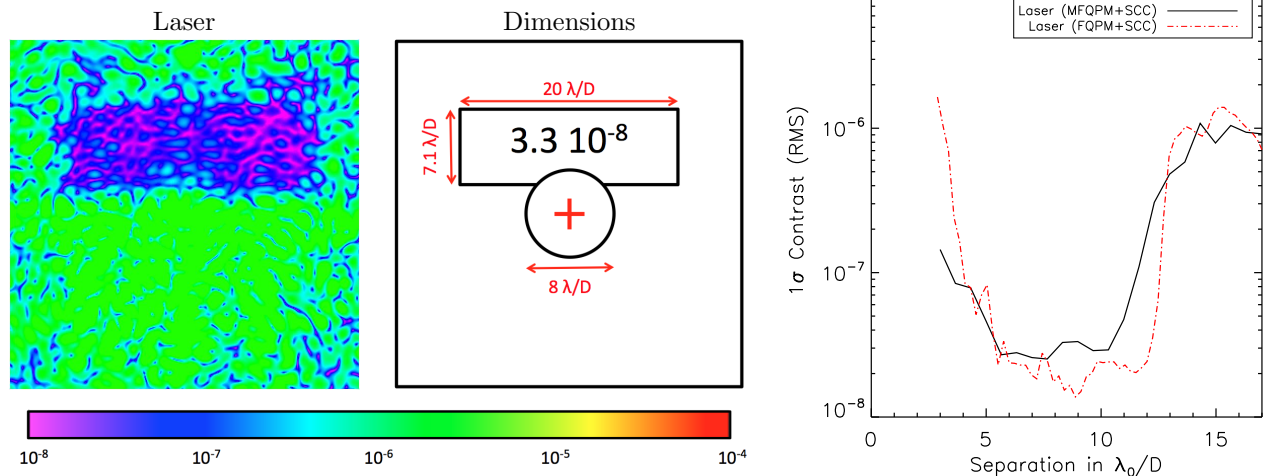
Figure 4. Left: experimental half dark hole (DH) obtained with the MFQPM+SCC in monochromatic light. The size of the image is 30 by 30 λ_0/D. Middle: dimensions of the DH. The red cross represents the optical axis. The standard deviation inside the half DH is 3.3 10^{-8}. Right: Associated 1σ contrast curve (black solide line) compared to the FQPM+SCC performance (red dashed line) computed inside the DH.

This experiment demonstrates two main results. First, the SCC works with an other coronagraph than the FQPM. This was expected from numerical sumulations but it is the first time that we demonstrate it in laboratory. Then, we prove that the MFQPM+SCC can reach contrast of 3 10^{-8} in monochroamtic light, which is close to the expected performance (§3.2.1).

Now, we test the performance of the MFQPM in all narrow filters (Table 1) following the procedure described in §3.1. Images and contrast curves are presented in Figure 5. For the filter 647-10, performance are very close to those obtained in monochromatic light. Indeed, as we can see on Figure 3, this filter and the monochromatic source are near to the optimal wavelength of the MFQPM (639 nm). For filters 620-10 and 660-10, the attenuation slightly degrades: $1-2\,10^{-7}$ between 5 and $10\lambda_0/D$. And for the filter 680-10, the performance strongly degrades: $\approx 4\,10^{-7}$ between 5 and $10\lambda_0/D$.

Finally, we test the MFQPM in wide filters. Results are shown in Figure 6. For the filter R22, the contrast obtained between 5 and $10\lambda_0/D$ is arround 7 10^{-8}, and for the filter R8, performance are slightly degraded: $\approx 10^{-7}$ for the same range of angular separations.

We summarize in Table 2, the standard deviation of the contrast inside the half DH described in Figure 4 for all the filters described in Table 1.

	Laser	620-10	647-10	660-10	680-10	R22	R8
1σ contrast into the half dark hole	3.3 10^{-8}	1.3 10^{-7}	3.9 10^{-8}	1.2 10^{-7}	5 10^{-7}	8.4 10^{-8}	1.4 10^{-7}

Table 2. Standard deviations inside the half DH obtained with a MFQPM for all the filters.

Our prototype of the MFQPM is thus less chromatic than the FQPM[9] but its performance are not as good as what we expected from numerical simulation (10^{-8} between 600 nm and 700 nm). Our prototype uses four lenses with small focal lengths to minimize the bulk of the instrument. We believe that one of the lenses was misaligned and that the beam was shifting with wavelength in a Lyot stop plane. Unfortunately, we could not adjust the position of this lens. As a result, one of the Lyot stop diaphragms was well aligned for a unique wavelength. Hence in polychromatic light, the coronagraph was not well aligned for the other wavelengths, which strongly degraded the performance.
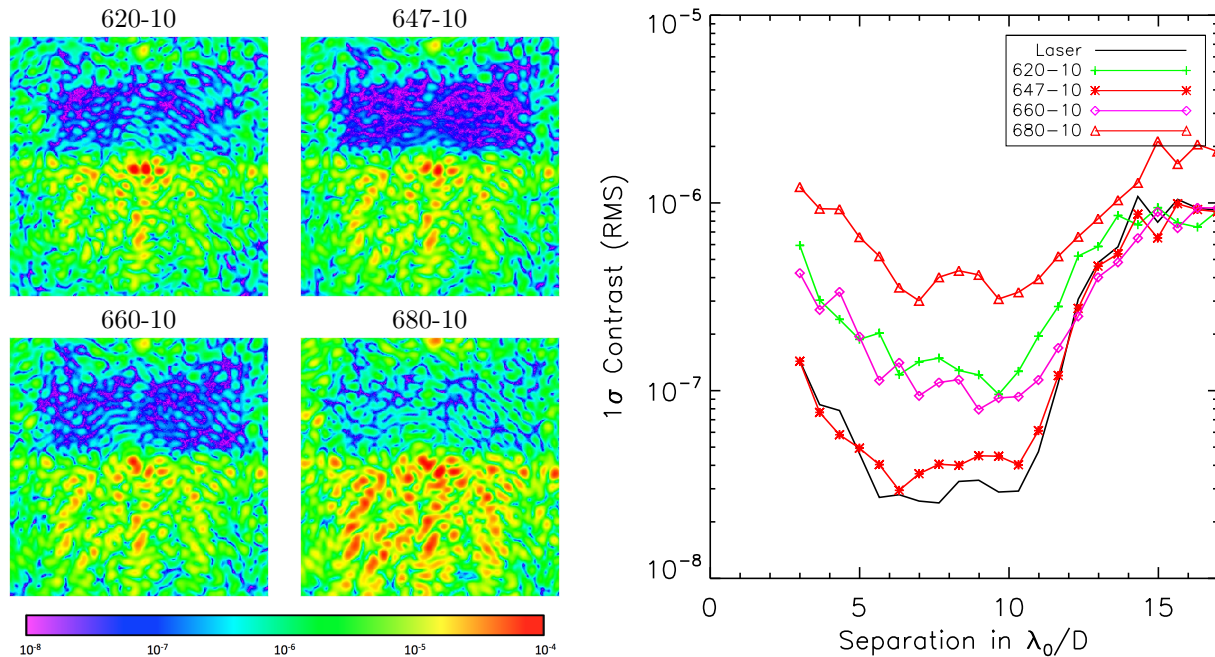
Figure 5. Left: the four images obtained in narrow bandpass filters (Table 1) with the MFQPM. We control the DM using the command obtained with MFQPM+SCC in monochromatic light. Right: Associated 1σ contrast curves compared to the performance obtained in monchromatic light (black solid line).
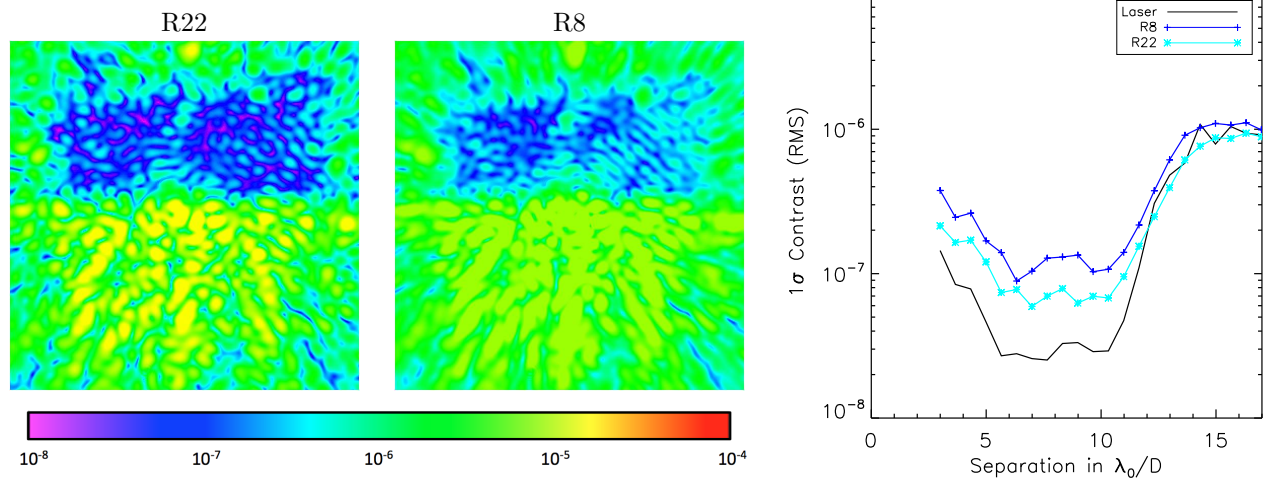

Figure 6. Left: the two images obtained in wide bandpass filters (Table 1) with the MFQPM. We control the DM using the command obtained with MFQPM+SCC in monochromatic light. Right: Associated 1σ contrast curves compared to the performance obtained in monochromatic light (black solid line).

3.3 DZPM

3.3.1 Brief reminder

The dual-zone phase mask (DZPM[17, 18]) is a generalization of the Roddier and Roddier[19] phase mask coronagraph for polychromatic observations. It is composed of an apodizer in a pupil plane (Fig. 7 left), a focal plane mask in a downstream focal plane (Fig. 7 middle) and a Lyot stop in the following pupil plane. The phase mask consists of two concentric rings (that induce different phase shifts). The prototype that we tested (Fig. 7) was optimised to reach contrasts of $\approx 10^{-8}$ between 5 and $10\lambda_0/D$ between $\lambda = 600$ nm and 700 nm. The spectra of the filters

used to tested our DZPM prototype are plotted in the Figure 7.

Figure 7. Left: Apodizer used with DZPM. Middle: DZPM phase mask. Right: Spectra used in our experiment.

3.3.2 Results and comments

We followed the same procedure as for the MFQPM (3.1).

First, contrasts obtained in monochromatic light using the DZPM+SCC configuration (Fig.8) are very similar to those obtained under the same conditions with the FQPM+SCC configuration. Indeed, contrasts reached are $1-3\ 10^{-8}$ between 6 and 12 λ_0/D. Thus, we prove that the SCC works with a third kind of coronagraph. The main dimensions of the half DH are given in Figure 8. The standard deviation inside this DH is $2.8\ 10^{-8}$. In this experiment, the diameter of our Lyot stop diaphragm is $\varnothing_L = 7.6$ mm when the entrance pupil is $\varnothing_P = 8$ mm. The diameter of the SCC reference is 0.3 mm and the distance between the optical axis and the center of this hole reference is $\xi = 1.9\ \varnothing_L$.
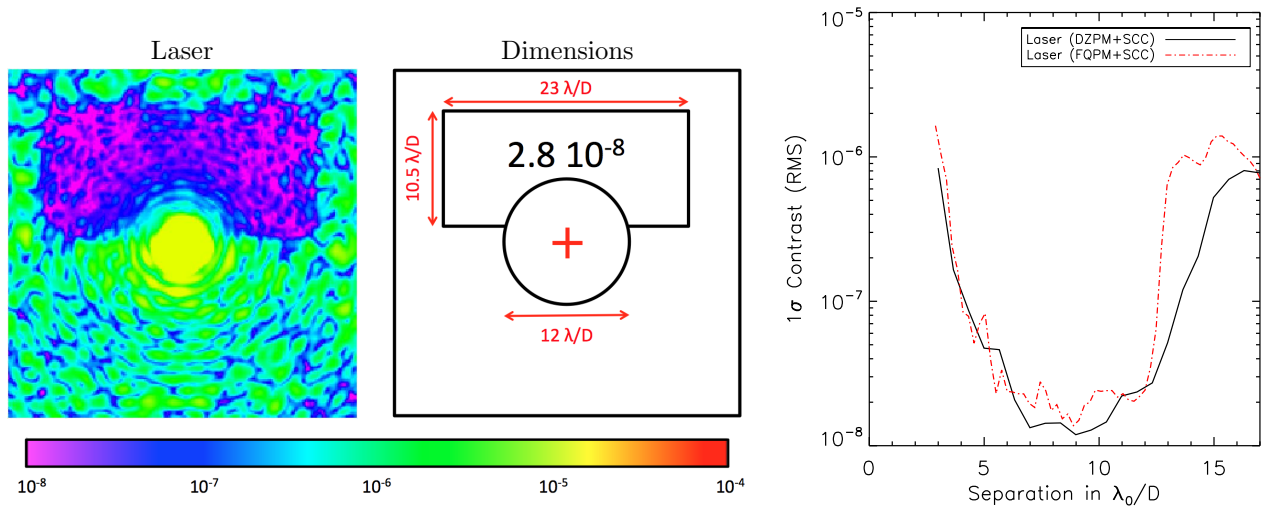

Figure 8. Left: experimental half dark hole (DH) obtained with the DZPM+SCC in monochromatic light. The size of this image is 30 by 30 λ_0/D. Middle: dimensions of the DH. The red cross represents the optical axis. The standard deviation inside the half DH is $2.8\ 10^{-8}$. Right: Associated 1σ contrast curve (black solide line) compared to the FQPM performance (red dashed line) computed inside the DH.

Then, we tested performance in all narrow filters. Images and results obtained are shown in Figure 9. In the case of the DZPM, the contrast is under $5\ 10^{-8}$ between 6 and $12\lambda_0/D$ for all filters. Moreover, for the R8 and

Proc. of SPIE Vol. 9151 91515Q-7

R22 wide filters (Figure 10), the prototype is achromatic enough to reach contrasts lower than $4\ 10^{-8}$ between 6 and $12\lambda_0/D$.
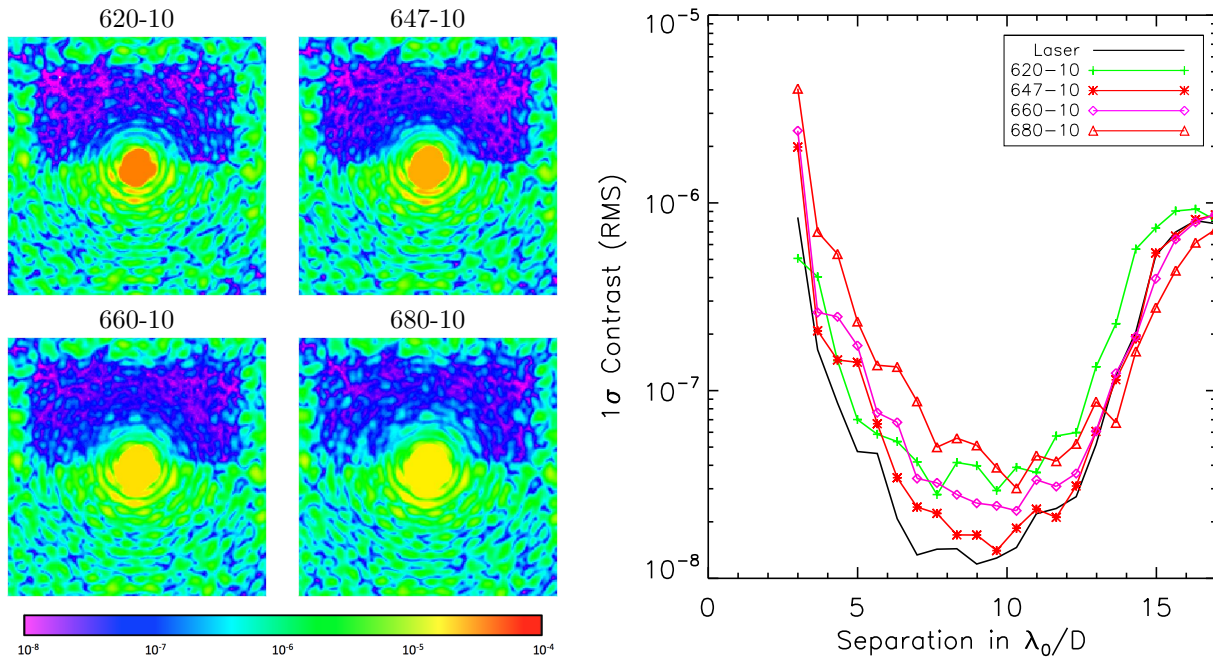

Figure 9. Left: the four images obtained in narrow bandpass filters (Table 1) with the DZPM. We control the DM using the command obtained with DZPM+SCC in monochromatic light. Right: Associated 1σ contrast curves compared to the performance obtained in monchromatic light (black solid line).

We summarize in Table 3, the standard deviations of the contrast inside the half DH for all the filters.
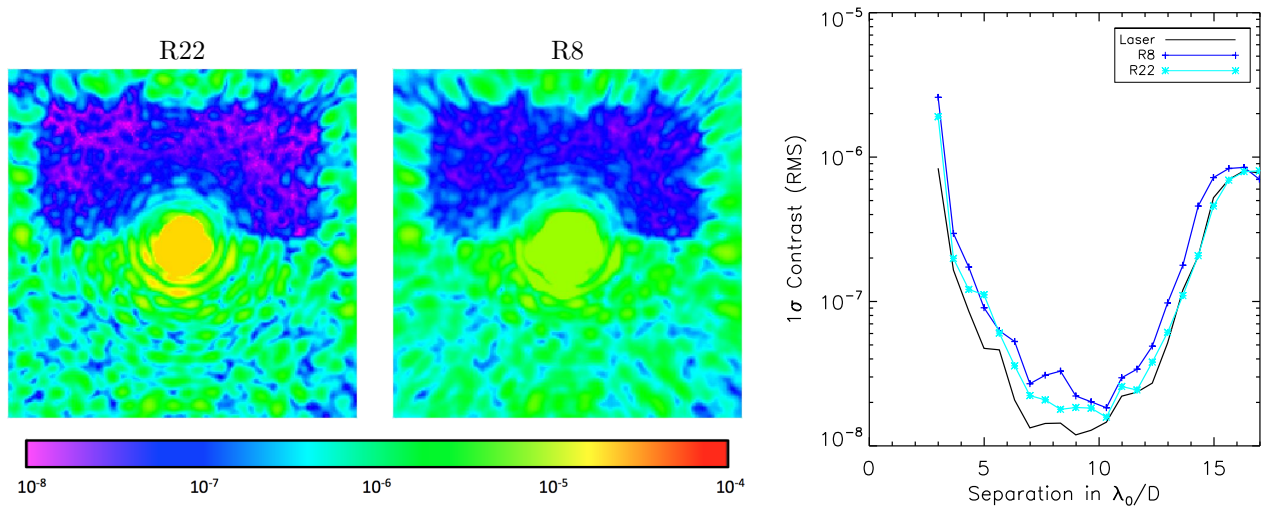

Figure 10. Left: the two images obtained in wide bandpass filters (Table 1) with the DZPM. We control the DM using the command obtained with DZPM+SCC in monochromatic light. Right: Associated 1σ contrast curves compared to the performance obtained in monchromatic light (black solid line).

We conclude that the performance of our DZPM prototype is as achromatic as expected. We also conclude that it is more achromatic than our MFQPM prototype.

	Laser	620-10	647-10	660-10	680-10	R22	R8
1σ contrast into the half dark hole	$2.8\ 10^{-8}$	$7.1\ 10^{-8}$	$3.4\ 10^{-8}$	$5\ 10^{-8}$	$9\ 10^{-8}$	$3.4\ 10^{-8}$	$4.3\ 10^{-8}$

Table 3. Standard deviations inside the half DH obtained with the DZPM for all the filters.

4. ACHROMATIC FOCAL PLANE WAVEFRONT SENSOR

The current version of the SCC is very sensitive to chromatism. Indeed, the SCC can estimate the electric field of the speckles only if they are spatially modulated by fringes. In monochromatic light, fringes are well contrasted in all the field of view (Fig 1, middle) whereas, in polychromatic light, because of the reduced temporal coherence of the star light, fringes get blurred in one direction and only part of the speckles are fringed (Fig 11, middle).
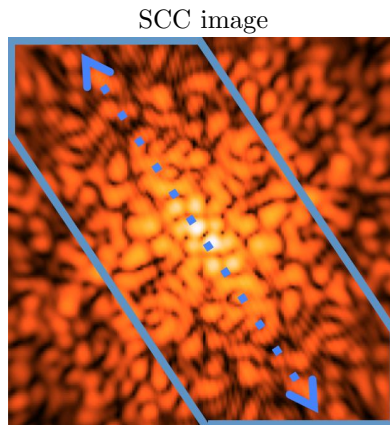
SCC image

Figure 11. SCC image in polychromatic light R=16.

So, in polychromatic light, only part of the DH can be corrected. To overcome this problem, we propose a new version of the SCC: the multi-reference SCC. In §4.1, we present the upgraded version of the SCC, that is expected to be more achromatic. Finally, we present laboratory performance that confirm the interest of the multi-reference SCC in §4.2.

To test the upgraded version of our focal plane wavefront sensor (SCC), we use the DZPM coronagraph that shows better performance in white light than the prototype of the MFQPM.

4.1 Multi-reference SCC

In order to improve the performance in polychromatic light, we modify the first version of the SCC by adding other reference holes in the Lyot Stop (Fig. 12, Left). Adding another reference generates interference fringes in the speckles like the first one but in an other direction (Fig. 12, Middle). The directions of the fringe patterns depend on the positions of the SCC reference holes. Each SCC reference hole generates a fringe pattern in the focal plane that get blurred because of chromatism in the direction perpendiculary to the fringe direction. By adding several references at chosen positions, the intensity of each speckle inside the DH can be spatially modulated by at least one of the fringe patterns. As we can see on the right of the Figure 12, each time we add a reference hole, a new couple of correlation peaks and small correlation peaks between the references appear in the Fourrier plane. In order to be able to exploit the maximum of the information contained in those peaks, we avoid overlaps between them, with the central autocorrelation peak and with the small correlation peaks.

So we optimize the position of each SCC reference hole in order to spatially modulate the maximum of speckles inside the half DH.
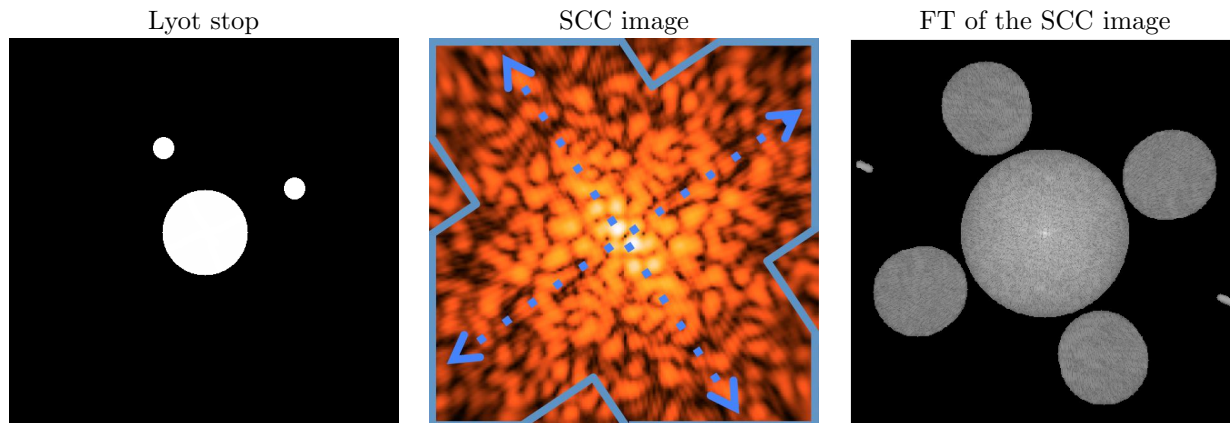
Figure 12. Left: Lyostop with two references. Middle: SCC image in polychromatic light R=16. Right: Fourier transform of the SCC image.
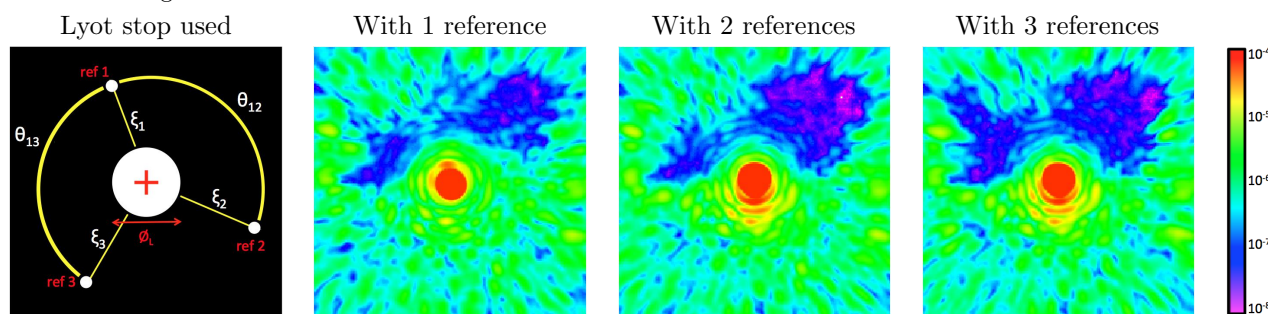

Figure 13. From left to right: Lyot stop and SCC reference holes. Correction with the reference 1, correction with the references 1 and 2, and correction with the 3 references. These images have been made with the association DZPM+Multi-reference SCC and the R8 filter. The size of the dark hole is 10.5 by $24\lambda_0/D$. The main dimensions of the Lyot stop are: the diameter of the diaphragm $\varnothing_L = 8$ mm, the diameter of all the references is $\varnothing_r = 0.3$ mm, the angles between the references $\theta_{12} = 135°$, $\theta_{13} = 130°$, the distances between the optical axis (red cross) and the center of each reference $\xi_1 = 1.76\,\varnothing_L$, $\xi_2 = 1.89\,\varnothing_L$ and $\xi_3 = 1.93\,\varnothing_L$.

4.2 Correction

In this section, we present the results obtained in a half DH in polychromatic light (R8 filter) using a DZPM coronagraph and a SCC with one, two or three SCC reference holes. Images of the best corrections for each case are showed in Figure 13. Size of the dark hole that we tried to correct is 10.5 by $23\lambda_0/D$.

On the left of the figure, we give the configuration and the main dimensions of the Lyot stop. Then, in the second image from the left, we did a correction using a DZPM + 1 reference SCC. During the correction there is only one pattern of fringes so only some speckles are modulated because of chromatism. The correction is not efficient and only a small part of the DH is corrected. Using two reference holes (Fig. 13, third image), we have two patterns of fringes in the SCC image. More speckles are spatially modulated. A larger part of the half DH is corrected. With three reference holes (Fig. 13, right), we use three patterns of fringes. More speckles are spatially modulated. The correction is better and the major part of the DH is corrected.

In Figure 14, we present the best correction that we obtained in polychromatic light (R=8) using the DZPM+ 3 reference SCC. Once again, in this figure, we give the main dimensions of the DH and the associated 1σ contrast curve. As we can see, in this configuration we can reach contrast of the order of $2-4\,10^{-8}$ between 5 by $12\lambda_0/D$. The performance is very similar to the monochromatic performance. In other words, we built a coronagraphic device associated to a focal plane wavefront sensor which can control a DM to reach $\approx 3\,10^{-8}$ contrast in polychromatic light (R=8).

In conclusion, the multi-reference SCC, associated to an achromatic coronagraph as DZPM, is a focal plane wavefront sensor which is capable to reach contrasts of the order of 10^{-8} at a few λ_0/D of the central star in a
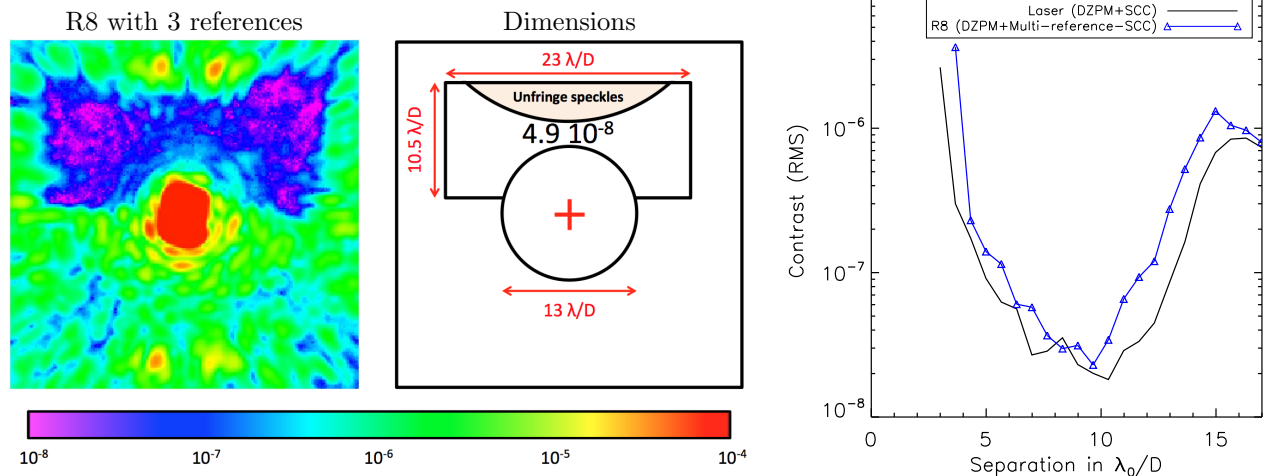
Figure 14. Left: experimental half DH obtained in polychromatic light (R8 filters) for the association DZPM+Multi-reference SCC. Middle: dimensions of the DH. Right: Associated 1σ contrast curve (black solid line) compared to the DZPM+SCC performance in monochromatic light (black line) computed inside the DH.

wide spectral band.

5. CONCLUSION

In conclusion, our laboratory experiments prove that the SCC works with other coronagraphs (MFQPM and DZPM) than FQPM. This was expected from numerical sumulations but it is the first time that we demonstrate it in laboratory. Then, we prove that MFQPM and DZPM can reach high-contrast in monochromatic light: $3 \ 10^{-8}$ between 5 and 10 λ_0/D for MFQPM and $1 - 3 \ 10^{-8}$ between 5 and 10 λ_0/D for DZPM. We also prove that our DZPM prototype is achromatic enough to reach contrasts lower than $4 \ 10^{-8}$ between 6 and $12\lambda_0/D$ over a $> 10\%$ bandpass.

Moreover, we have improved the SCC. The new version of the SCC, with several SCC reference holes into the Lyot stop, is more achromatic. In fact, we can suppress the speckles inside the DH to reach 10^{-8} contrast at a few λ_0/D of the central star over a $> 10\%$ bandpass.

The current limitations are the amplitude aberrations with low spatial frequencies and the uncorrected speckles outside the DH.

To enhance the size and contrast level of the DH, we will study two news improvements:

- In order to reduce the light that is diffracted inside the DH by speckles that are outside the DH, we will test a post coronagraphic apodizer.

- We will implement two more DM to correct for both amplitude and phase aberrations and create a full DH.[20]

ACKNOWLEDGMENTS

REFERENCES

[1] Marois, C., Macintosh, B., Barman, T., Zuckerman, B., Song, I., Patience, J., Lafrenière, D., and Doyon, R., "Direct Imaging of Multiple Planets Orbiting the Star HR 8799," *Science* **322**, 1348– (Nov. 2008).

[2] Marois, C., Zuckerman, B., Konopacky, Q. M., Macintosh, B., and Barman, T., "Images of a fourth planet orbiting HR 8799," *Nature* **468**, 1080–1083 (Dec. 2010).

[3] Lagrange, A.-M., Kasper, M., Boccaletti, A., Chauvin, G., Gratadour, D., Fusco, T., Ehrenreich, D., Apai, D., Mouillet, D., and Rouan, D., "Constraining the orbit of the possible companion to β Pictoris. New deep imaging observations," *Astronomy and Astrophysics* **506**, 927–934 (Nov. 2009).

[4] Konopacky, Q. M., Barman, T. S., Macintosh, B. A., and Marois, C., "Detection of Carbon Monoxide and Water Absorption Lines in an Exoplanet Atmosphere," *Science* **339**, 1398–1401 (Mar. 2013).

[5] Bordé, P. J. and Traub, W. A., "High-Contrast Imaging from Space: Speckle Nulling in a Low-Aberration Regime," *Astrophysical Journal* **638**, 488–498 (Feb. 2006).

[6] Baudoz, P., Boccaletti, A., Baudrand, J., and Rouan, D., "The Self-Coherent Camera: a new tool for planet detection," in [*IAU Colloq. 200: Direct Imaging of Exoplanets: Science Techniques*], Aime, C. and Vakili, F., eds., 553–558 (2006).

[7] Galicher, R., Baudoz, P., Rousset, G., Totems, J., and Mas, M., "Self-coherent camera as a focal plane wavefront sensor: simulations," *Astronomy and Astrophysics* **509**, A31 (Jan. 2010).

[8] Mazoyer, J., Baudoz, P., Galicher, R., Mas, M., and Rousset, G., "Estimation and correction of wavefront aberrations using the self-coherent camera: laboratory results," *Astronomy and Astrophysics* **557**, A9 (Sept. 2013).

[9] Mazoyer, J., Baudoz, P., Galicher, R., and Rousset, G., "High-contrast imaging in polychromatic light with the self-coherent camera," *Astronomy and Astrophysics* **564**, L1 (Apr. 2014).

[10] Rouan, D., Riaud, P., Boccaletti, A., Clénet, Y., and Labeyrie, A., "The Four-Quadrant Phase-Mask Coronagraph. I. Principle," *Publications of the Astronomical Society of the Pacific,* **112**, 1479–1486 (Nov. 2000).

[11] Galicher, R., Baudoz, P., and Rousset, G., "Wavefront error correction and Earth-like planet detection by a self-coherent camera in space," *Astronomy and Astrophysics* **488**, L9–L12 (Sept. 2008).

[12] Mas, M., Baudoz, P., Mazoyer, J., Galicher, R., and Rousset, G., "Experimental results on wavefront correction using the self-coherent camera," in [*Society of Photo-Optical Instrumentation Engineers (SPIE) Conference Series*], *Society of Photo-Optical Instrumentation Engineers (SPIE) Conference Series* **8446** (Sept. 2012).

[13] Abe, L., Domiciano de Souza, Jr., A., Vakili, F., and Gay, J., "Phase Knife Coronagraph. II - Laboratory results," *Astronomy and Astrophysics* **400**, 385–392 (Mar. 2003).

[14] Boccaletti, A., "Numerical Simulations for Coronagraphy. part II.," in [*EAS Publications Series*], Aime, C. and Soummer, R., eds., *EAS Publications Series* **12**, 165–176 (2004).

[15] Baudoz, P., Galicher, R., Baudrand, J., and Boccaletti, A., "Theory and laboratory tests of the multi-stage phase mask coronagraph," in [*Society of Photo-Optical Instrumentation Engineers (SPIE) Conference Series*], *Society of Photo-Optical Instrumentation Engineers (SPIE) Conference Series* **7015** (July 2008).

[16] Galicher, R., Baudoz, P., and Baudrand, J., "Multi-stage four-quadrant phase mask: achromatic coronagraph for space-based and ground-based telescopes," *Astronomy and Astrophysics* **530**, A43 (June 2011).

[17] Soummer, R., Dohlen, K., and Aime, C., "Achromatic dual-zone phase mask stellar coronagraph," *Astronomy and Astrophysics* **403**, 369–381 (May 2003).

[18] N'Diaye, M., Dohlen, K., Cuevas, S., Soummer, R., Sánchez-Pérez, C., and Zamkotsian, F., "Improved achromatization of phase mask coronagraphs using colored apodization," *Astronomy and Astrophysics* **538**, A55 (Feb. 2012).

[19] Roddier, F. and Roddier, C., "Stellar Coronograph with Phase Mask," *Publications of the Astronomical Society of the Pacific,* **109**, 815–820 (July 1997).

[20] Galicher, R., Baudoz, P., Delorme, J.-R., Mazoyer, J., Rousset, G., Firminy, J., Boussha, F., N'Diaye, M., Dohlen, K., and Caillat, A., "High-Contrast imaging on the THD bench: porgress and upgrate," in [*Society of Photo-Optical Instrumentation Engineers (SPIE) Conference Series*], *Society of Photo-Optical Instrumentation Engineers (SPIE) Conference Series* (2014).